

This article was downloaded by:[Tufts University]
[Tufts University]

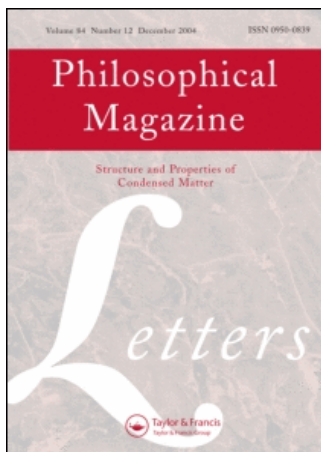
On: 24 March 2007

Access Details: [subscription number 731636168]

Publisher: Taylor & Francis

Informa Ltd Registered in England and Wales Registered Number: 1072954

Registered office: Mortimer House, 37-41 Mortimer Street, London W1T 3JH, UK



Philosophical Magazine Letters

Publication details, including instructions for authors and subscription information:

<http://www.informaworld.com/smpp/title-content=t713695410>

Superheating of bulk polycrystalline selenium

H. Lu; N. X. Sun; Y. C. Zhou; Y. F. Wang

To cite this Article: H. Lu, N. X. Sun, Y. C. Zhou and Y. F. Wang, 'Superheating of bulk polycrystalline selenium', *Philosophical Magazine Letters*, 76:1, 49 - 56

xxxx:journal To link to this article: DOI: 10.1080/095008397179372

URL: <http://dx.doi.org/10.1080/095008397179372>

Full terms and conditions of use: <http://www.informaworld.com/terms-and-conditions-of-access.pdf>

This article maybe used for research, teaching and private study purposes. Any substantial or systematic reproduction, re-distribution, re-selling, loan or sub-licensing, systematic supply or distribution in any form to anyone is expressly forbidden.

The publisher does not give any warranty express or implied or make any representation that the contents will be complete or accurate or up to date. The accuracy of any instructions, formulae and drug doses should be independently verified with primary sources. The publisher shall not be liable for any loss, actions, claims, proceedings, demand or costs or damages whatsoever or howsoever caused arising directly or indirectly in connection with or arising out of the use of this material.

© Taylor and Francis 2007

Superheating of bulk polycrystalline selenium

By H. LU, N. X. SUN, Y. C. ZHOU

Institute of Metal Research, Chinese Academy of Sciences, Shenyang 110015,
PR China

and Y. F. WANG

China National Ordnance Bureau, Beijing 100086, PR China

[Received 2 January 1997 and accepted 14 April 1997]

ABSTRACT

A superheating of 5°C has been observed in bulk polycrystalline selenium with a mean grain size of about 10 µm. The superheating is interpreted on the basis of the unique grain boundary structure inside the Se samples, which gives rise to a free energy barrier to liquid nuclei formation in the grain boundaries.

Superheating is a rare phenomenon; most solids, especially metals, are found to melt on heating at the equilibrium melting point T_0 . The conventional explanation to this melting phenomenon is that most liquids can effectively wet their own solids, i.e.

$$\gamma_{sl} + \gamma_{lv} \leq \gamma_{sv} \quad (1)$$

where γ_{sl} , γ_{lv} and γ_{sv} are the interfacial free energies of the solid–liquid, liquid–vapour and solid–vapour interfaces respectively. Therefore the wetting angle $\theta = 0$ and no superheating is required for liquid nucleation. Most superheating phenomena have been observed in embedded/coated particles with an epitaxial relationship between the contained solid and the matrix (Rossouw and Donnelly 1985, Daeges, Gleiter and Perepezko 1986, Evans and Mazey 1986), and it is possible that an incoherent interface might not permit substantial superheating (Cahn 1986). However, for some solids which melt into viscous liquids with sluggish melting kinetics, substantial superheating levels have been observed, ranging up to 450°C for quartz, but this approach is limited to some network-forming materials (Ainslie, Mackenzie and Turnbull 1961, Uhlmann 1980).

There have been many papers dealing with the upper limiting temperature for superheating of crystals (Uhlmann 1980, Fecht and Johnson 1988, Lele, Ramachandrarao and Dubey 1988, Cahn 1989, Tallon 1989) although experimental investigations on the superheating behaviour of solids, especially bulk solids, are comparatively scarce.

Until recently it was believed to be impossible to superheat a crystal above its melting point except by arranging to heat a solid from the interior (Cormia, Mackenzie and Turnbull 1963). Even then the attainable superheating was very small, about 2°C for tin (Khaikin and Bene 1939). This idea was disproved by an experiment (Daeges *et al.* 1986) in which a superheating of 24 K was observed in small (about 0.15 mm) silver monocrystal spheres coated with gold. Superheating in elements surrounded by their own vapour has been observed only in thin platelets

(about 100 nm) of bismuth and lead monocrystals with specific low-index free surfaces. In these cases the superheating was believed to be caused by the presence of a nucleation barrier in forming the liquid on the low-index free surfaces, the attained superheating being higher when the particle became more faceted (Peppiatt and Sambles 1975, Spiller 1982). Superheating in bulk polycrystalline solids has never been reported to the knowledge of the author.

Here we report on the superheating of bulk polycrystalline selenium. The observed superheating was evidently not caused by a viscous melt propagating into the solid with sluggish melting kinetics. Rather it was caused by the presence of a nucleation barrier in liquid nuclei formation.

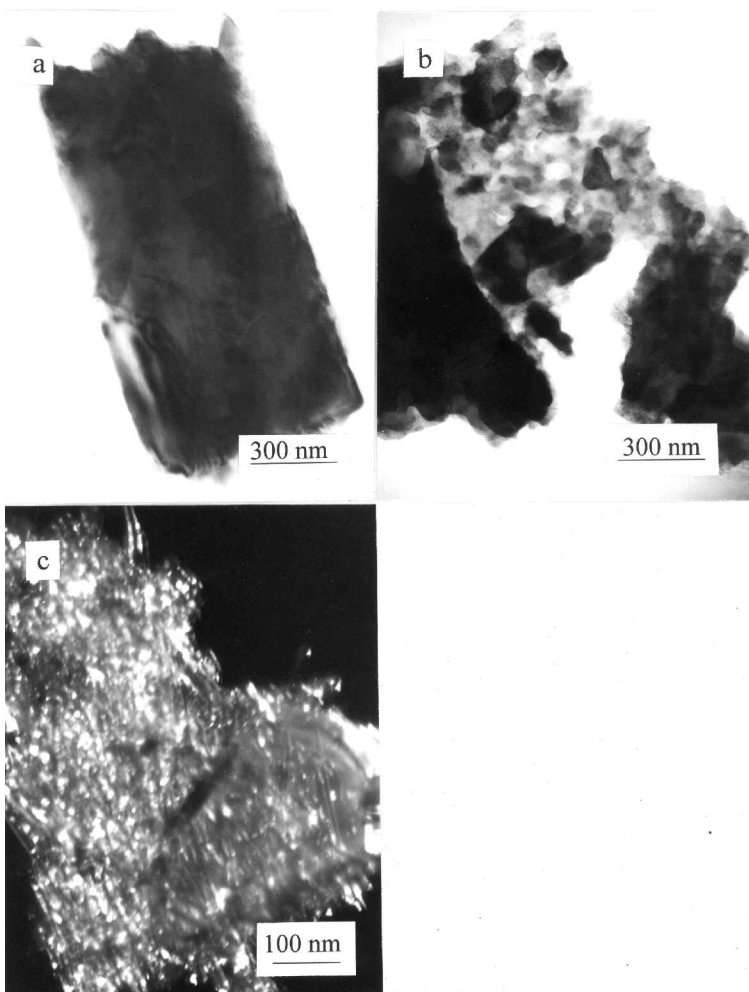
The synthesis route for the polycrystalline trigonal selenium in bulk form is as follows. First, commercial amorphous Se (with a purity of 99.999%) was sealed in a quartz tube (about 10 mm in diameter) which was evacuated to about 10^{-5} Torr. The Se was melted for 2 h at 400°C, then kept at $210 \pm 10^\circ\text{C}$ for 3.6×10^6 s (sample A) and for 3.6×10^5 s (sample B) respectively. The melt was then cooled to room temperature in the furnace. For the purpose of comparison, crystalline Se samples were synthesized by completely crystallizing amorphous Se at 100°C for 280 min (sample C); details for the synthesis route can be found in Sun and Lu (1996). A Rigaku X-ray diffractometer (D/max-rA), and a Philips EM420 transmission electron microscope were utilized to determine the mean grain size and microstructure of the samples A, B and C. The bulk Se samples were pulverized into powders and deposited on a copper grid in alcohol for transmission electron microscopy (TEM) observation. A scanning electron microscope (JSM-6301F) was used to examine the fracture surfaces of the Se samples, and a surface analysis system (LAS-3000, Riber) was used to examine the impurity content at the fracture surface.

Melting experiments were carried out in a differential scanning calorimeter (DSC-7, Perkin-Elmer) under a flowing high purity argon atmosphere. The temperature and energy scales of differential scanning calorimeter were calibrated using pure Zn and In with accuracies of ± 0.1 K for temperature and ± 0.02 mJ for energy measurements. The sizes of the Se samples for differential scanning calorimetry (DSC) measurements were about 5 mm \times 5 mm \times 1 mm, which ensured good thermal contact between the sample and crucible.

Figures 1(a) and (b) show typical transmission electron micrographs of samples A and B respectively. A large monocrystal can be clearly seen in fig. 1(a), implying that the mean grain size in sample A may be in the range of at least a few micrometres. Figure 1(b) shows equiaxed crystalline grains with a mean grain size of about 100 nm. A transmission electron micrograph of sample C is shown in fig. 1(c), from which fibre-like grains with a diameter of several nanometres can be seen. X-ray diffraction (XRD) results show that only diffraction peaks for the trigonal Se phase are present in the XRD patterns of these Se samples, and the mean grain sizes for sample A and B are both larger than 100 nm, while the mean grain size for sample C is about 10 nm. The XRD results on the mean grain size correspond well with the TEM results.

Scanning electron microscopy (SEM) observations on the fracture surfaces of samples A, B and C were carried out. Figures 2(a) and (b) show typical scanning electron micrographs of the fracture surfaces of the peripheral part and the core part respectively of sample A. It can be clearly seen that sample A is not uniform, the core part being comparatively denser than the peripheral part. The peripheral part of sample A shows clearly the intergranular fracture surface, and grain boundaries can

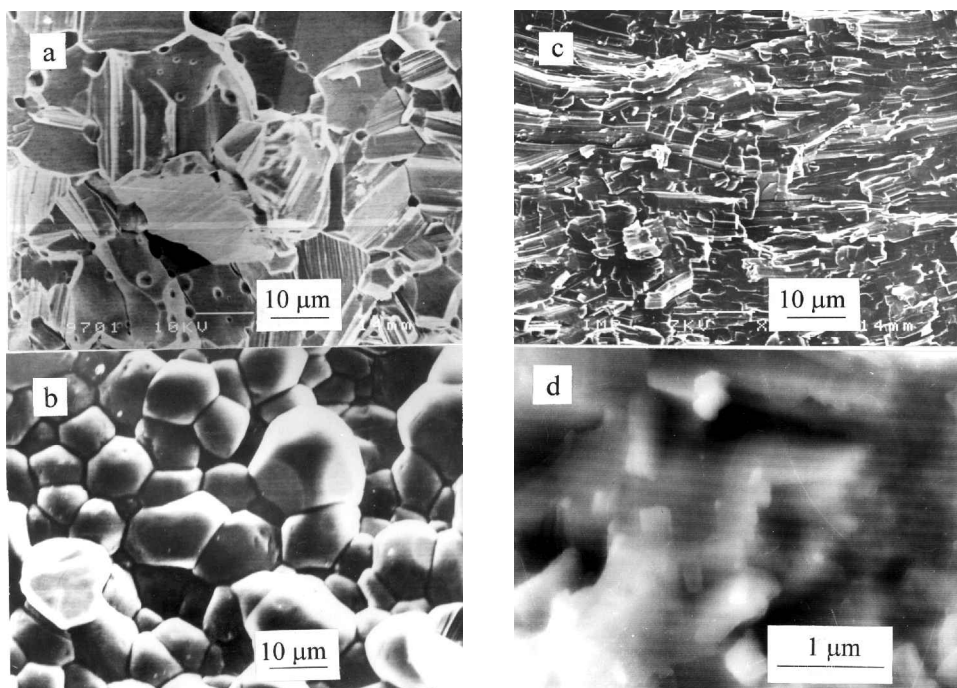
Fig. 1



TEM images of the Se samples: (a) sample A, (b) sample B and (c) sample C.

be clearly seen with a mean grain size of about $10\ \mu\text{m}$. Furthermore, near-spherical pores with a diameter of about $1\text{--}10\ \mu\text{m}$ can be found in the grain boundaries, triple junctions and inside the crystallite grains. However, the core part of sample A shows clearly the intragranular fracture surface, the whole of protruding polyhedron-shaped crystallite grains with a mean grain size of about $10\ \mu\text{m}$ can be clearly seen, and the boundaries are rather flat. The scanning electron micrograph of the fracture surface of sample B is shown in fig. 2(c), from which laminar steps can be clearly seen, exhibiting typical intergranular fracture surfaces. Figure 2(d) shows a scanning electron micrograph of the fracture surface of sample C; broken rectangular bars with even fracture surfaces can be clearly seen, also indicating intergranular fracture. All the Se samples show intergranular fracture surfaces as observed previously in trigonal Se (Fitton and Griffiths 1968, Zhang, Hu and Lu 1995), except the core part of sample A, which exhibits a typical intragranular fracture surface.

Fig. 2

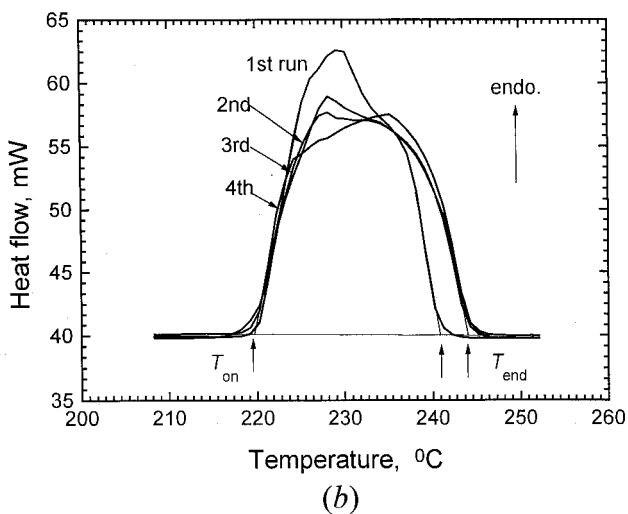
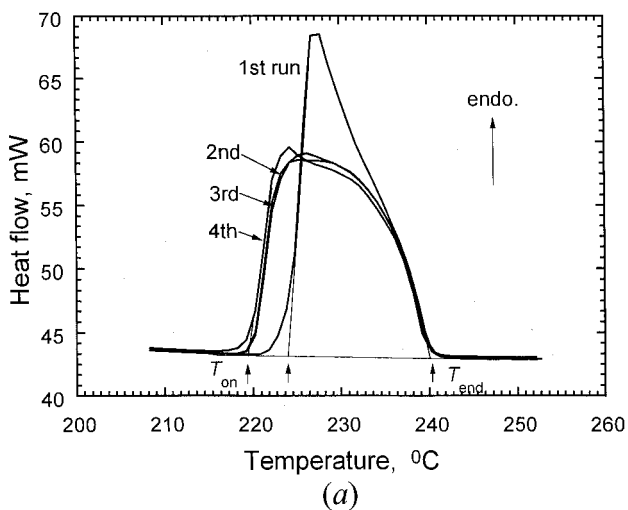


Scanning electron micrographs of the fracture surfaces of the Se samples: (a) peripheral part of sample A, (b) core part of sample A, (c) sample B and (d) sample C.

Results of Auger electron microscopy show that there are no impurities such as oxygen and nitrogen on any of the fracture surfaces of these Se samples.

The melting behaviour of the three samples was investigated calorimetrically. Dynamic DSC analyses on the melting behaviour were performed in the temperature range 100–260°C at a heating rate of 10 K min⁻¹. What is interesting is that the core part of sample A shows very different melting behaviour from those of samples B and C, while the melting behaviour of the peripheral part of sample A is rather similar to those of samples B and C. The DSC curves on the peripheral and core parts of sample A are indicated in figs. 3(a) and (b) respectively. When first heated, the core part of sample A melts at an onset temperature of 224.4°C ($T_{\text{on}} = 224.4^\circ\text{C}$, as illustrated in fig. 3(a)). But after the sample is heated to 260°C, cooled down to 100°C and reheated, it melts at a nearly constant onset temperature of $219.3 \pm 0.3^\circ\text{C}$, which is 5.1°C lower than the melting temperature in the first run. The melting temperature in the following three runs, being $219.3 \pm 0.3^\circ\text{C}$, coincides well with 220°C, the literature value for the equilibrium melting point of Se (Hultgren *et al.* 1973). The integrated enthalpy of fusion of the core part of sample A was nearly constant for the four runs, and is $6180 \pm 80 \text{ J mol}^{-1}$, which is also in agreement with the literature value for Se (Hultgren *et al.* 1973). The peripheral part of sample A melts at a nearly constant onset temperature of $219.7 \pm 0.2^\circ\text{C}$ and the enthalpy of fusion was also constant in the four runs, namely $6140 \pm 80 \text{ J mol}^{-1}$. The latter two values coincide well with the literature values for Se (Hultgren *et al.* 1973). It is notable that the end temperature T_{end} (as illustrated in fig. 3(a)), for the core part

Fig. 3



Four dynamic DSC runs for melting processes of the Se samples: (a) core part of sample A, (b) peripheral part of sample A. The temperature–time programs for the four runs are identical, with a temperature range of $100^{\circ}\text{C} \leftrightarrow 260^{\circ}\text{C}$, heating rate of 10 K min^{-1} , and cooling rate of -200 K min^{-1} .

of sample A is 240.2°C and was nearly constant for the four runs, while the T_{end} values for the peripheral part of sample A are different in the four runs, with $T_{\text{end}} = 241.2^{\circ}\text{C}$ for the first run, and $T_{\text{end}} = 244.5^{\circ}\text{C}$ for the following three runs. The DSC curves for the melting process of samples B and C are similar to that of the peripheral part of sample A, their melting temperature being $219.6 \pm 0.5^{\circ}\text{C}$. The melting behaviour observed in samples B and C, and the peripheral part of sample A is similar to that previously observed for trigonal Se (Murphy, Altman and Wunderlich 1977, Zhang *et al.* 1995).

When first heated, the core part of sample A melts at an onset temperature of 224.4°C , which is 5.1°C higher than the measured melting temperature in the subsequent three runs and 4.4°C higher than the literature value for the equilibrium melting temperature for Se (Hultgren *et al.* 1973). The observed melting temperature elevation for the core part of sample A is evidently not caused by thermal lag. The peripheral part of sample A, and samples B and C all melt at the equilibrium melting point, and no thermal lag exists in the melting process of these Se samples. So, the measured temperature is the real temperature attained in the Se samples, and the core part of sample A can be superheated up to an onset temperature of 224.4°C , about 5°C higher than the equilibrium melting temperature for the other Se samples.

It is quite unusual that an evident superheating of about 5°C was observed in the bulk polycrystalline Se samples with a mean grain size of about $10\ \mu\text{m}$. The core and peripheral parts of sample A, with nearly identical thermal history and mean grain sizes, exhibit distinctly different fracture surfaces and distinctly different melting behaviours.

Selenium has a high glass forming ability. Liquid Se is composed of long linear chains and eight-atom rings (Andrievskii, Nabitovich and Voloshchuk 1960, Lucovsky, Mooradian, Taylor, Wright and Keezer 1967), while trigonal Se is composed of linear chains. It is true that materials tend to have a high glass forming ability when they melt into viscous liquids with sluggish melting kinetics, and the melting process of some of these materials is dominated by interface kinetics even at substantial degrees of superheating (Ainslie *et al.* 1961, Uhlmann 1980). However, the melting process of Se is not dominated by interface kinetics, as in some previous cases of superheating (Ainslie *et al.* 1961, Uhlmann 1980). The reason is as follows. Samples B and C and the peripheral part of sample A all melt at the equilibrium melting point, with no superheating effect, while the core part of sample A shows an evident superheating of 5°C . In particular, both the peripheral part and the core part of sample A have the same thermal history and nearly the same mean grain size. If the melting process of Se is caused by interface kinetics, then both the peripheral and core parts of sample A should exhibit similar melting behaviour. Therefore, the superheating effect observed in the melting process of the core part of sample A is not controlled by interface kinetics.

The reason that metastable superheated solids can be sustained for a measurably long time is that there exist free energy barriers impeding the transformation of the metastable superheated state into the stable liquid state. Generally, two kinds of free energy barriers are involved in the melting process, namely, the free energy barrier to liquid nuclei formation and the free energy barrier to liquid–solid interface movement (Ostwald 1910, Sun, Lu and Zhou 1997). As discussed above, the melting process of Se is not dominated by interface kinetics, i.e. liquid–solid interface movement. So, a free energy barrier to liquid nuclei formation may be responsible for the superheating of the core part of sample A.

SEM observations show that the core part of sample A shows a characteristic intragranular fracture surface, while the peripheral part of sample A, and samples B and C all show intergranular fracture surfaces. As the grain boundary structure is an important factor dominating the fracture mode in an element material, so the different fracture manner implies that the core part of sample A may assume a grain boundary structure which is different from those of the other Se samples. As it has been widely accepted that melting of solids often involves nucleation of liquids at

extended defects, such as grain boundaries, free surfaces, voids or dislocations (Cahn 1989, Wolf 1990), the relation between the melting process and the fracture mode in the Se samples may lead one to contemplate that differences in grain boundary structure may account for differences in the melting behaviour of these Se samples.

Peppiatt and Sambles (1975) investigated the melting behaviour of three types of bismuth particles, which were prepared under different deposition conditions. They found that a time delay was present in the melting process of each case; in particular a thin platelet form of Bi particles with extensive {0001} faces can be superheated up to 7 K higher than the bulk melting point. Similar superheating behaviour was also observed in lead by Spiller (1982). These authors attributed the superheating to the presence of a nucleation barrier in forming the liquid on the surfaces. Here, as observed in fig. 2(a), the fracture surface of the core part of sample A shows a unique intragranular fracture surface and also a unique grain boundary structure—the protruding polyhedral crystallite grains can be observed with rather flat boundaries. These flat boundaries may be reasonably expected to be in a low energetic state and to give rise to free energy barrier to liquid nuclei formation, thus making superheating possible.

In conclusion, we have observed an evident superheating of 5°C in bulk polycrystalline selenium with a mean grain size of about 10 μm. The superheating was not caused by sluggish melting kinetics, but rather, appears to be associated with the unique grain boundary structure inside the Se samples.

ACKNOWLEDGMENTS

The Chinese Academy of Sciences is gratefully acknowledged.

REFERENCES

- AINSLIE, G., MACKENZIE, J. D., and TURNBULL, D. J., 1961, *J. chem. Phys.*, **65**, 1718.
 ANDRIEVSKII, A. I., NABITOVICH, I. D., and VOLOSHCHUK, YA. V., 1960, *Sov. Phys. Crystallog.*, **5**, 349.
 CAHN, R. W., 1986, *Nature*, **323**, 668; 1989, *Ibid.*, **342**, 619.
 CORMIA, R. L., MACKENZIE, J. D., and TURNBULL, D. J., 1963, *J. appl. Phys.*, **34**, 2239.
 DAEGES, J., GLEITER, H., and PEREPEZKO, J. H., 1986, *Phys. Lett. A*, **119**, 79.
 EVANS, J. H., and MAZEY, D. J., 1986, *J. nucl. Mater.*, **138**, 176.
 FECHT, H. J., and JOHNSON, W. L., 1988, *Nature*, **336**, 567.
 FITTON, B., and GRIFFITHS, C. H., 1968, *J. appl. Phys.*, **39**, 3663.
 HULTGREN, R., DESAI, P. D., HAWKINS, D. T., GLESIER, M., KELLEY, K. K., and WAGMAN, D. D., 1973, *Selected Values of the Thermodynamic Properties of Elements* (Metals Park, Ohio: American Society for Metals).
 KHAIKIN, S. E., and BENE, N. R., 1939, *Acad. Sci. URSS*, **23**, 31.
 LELE, S., RAMACHANDRARAO, P., and DUBEY K. S., 1988, *Nature*, **336**, 567.
 LUCOVSKY, G., MOORADIAN, A., TAYLOR, W., WRIGHT, G. B., and KEEZER, R. C., 1967, *Solid State Commun.*, **5**, 113.
 MURPHY, K. E., ALTMAN, M. B., and WUNDERLICH, B., 1977, *J. appl. Phys.*, **48**, 4122.
 OSTWALD, W., 1910, *Lehrbuch der Allgemeinen Chemie*, Vol. II/1 (Leipzig: W. Englemann), p. 514.
 PEPIATT, S. J., and SAMBLES, J. R., 1975, *Proc. R. Soc. A*, **345**, 387.
 ROSSOUW, C. J. and DONNELLY, S. E., 1985, *Phys. Rev. Lett.*, **55**, 2960.
 SPILLER, G. D. T., 1982, *Phil. Mag. A*, **46**, 535.
 SUN, N. X., and LU, K., 1996, *Phys. Rev. B*, **54**, 6058.

- SUN, N. X., LU, H., and ZHOU, Y. C., 1997, *Phil. Mag. Lett.* (in the press).
- TALLON, J. L., 1989, *Nature*, **342**, 658.
- UHLMANN, D. R., 1980, *J. non-crystalline Solids*, **41**, 347.
- WOLF, D., 1990, *Surface Sci.*, **226**, 389.
- ZHANG, H. Y., HU, Z. Q., and LU, K., 1995, *Nanostruct. Mater.*, **5**, 41.